Gas Transport Properties of Polyarylates: Substituent Size and Symmetry Effects

M. R. Pixton and D. R. Paul*

Department of Chemical Engineering and Center for Polymer Research, The University of Texas at Austin, Austin, Texas 78712

Received February 28, 1995; Revised Manuscript Received September 11, 1995[⊗]

ABSTRACT: Gas transport of helium, hydrogen, oxygen, nitrogen, methane, and carbon dioxide gases in a series of polyarylates based on isophthalic acid has been examined. These polyarylates were prepared from dimethyl-Bisphenol A, tetramethyl-Bisphenol A, diisopropyl-Bisphenol A, and dibromodimethyl-Bisphenol A monomers to study the effects of varying Bisphenol substituent group size, symmetry, and polarity. Symmetrical placement of substituent groups increases permeability while asymmetrical placement lowers permeability. Substitution of a tertiary butyl group at position 5 on the isophthalate ring increases polymer permeability. Most of the increases in permeability can be related to increases in the diffusion coefficients of all the gases. The isophthalate of dibromodimethyl-Bisphenol A has gas separation properties very similar to those of the tetrabrominated analog.

Introduction

The growth of commercial membrane-based gas separation processes has been fueled to some extent by the development of improved membrane materials. There is now extensive literature detailing the relationships between gas transport properties and polymer structure.[1–21] The goal of current research efforts is to identify new materials which are simultaneously more permeable and more selective and which, hopefully, exceed the "upper bound" in the relation between selectivity and permeability, as identified by Robeson,[22] of presently known polymers.

Previous studies of structure/property relationships have identified various guidelines for the design of improved gas separation membrane materials. Some authors have suggested that structural changes which both inhibit chain packing and reduce rotational mobility around flexible linkages in the polymer backbone might lead to higher permselectivity without a loss in permeability.[8,23,24] For aromatic polymers, the rotation of phenyl rings around their connecting bond axis is the primary rotational motion which can be inhibited. Small group substitutions on these phenyl rings is one way of reducing their rotational mobility and of, simultaneously, inhibiting close chain packing. The degree of such rotational inhibition can be qualitatively judged by observing shifts in the temperature at which sub-T_g relaxations occur or from the magnitude of the relaxation peaks while the inhibition of chain packing can be evaluated from density, d spacing, and fractional free volume measurements.

The placement symmetry of small group substitutions on polymer phenyl rings can have a marked effect on the gas transport as well as other physical properties of the substituted material.[3,6] Two types of phenyl ring substitution symmetry/asymmetry are shown in Figure 1. Type A asymmetry refers to a monosubstituted versus a disubstituted phenyl ring, where the substituent is the same in each case. Type B asymmetry refers to a disubstituted phenyl ring where the two substituents are not identical. Effects of type A asymmetry on gas transport properties are expected to be much greater than those of type B asymmetry. Symmetrically substituted polymers generally have higher permeabilities and lower selectivities than their unsubstituted analogs while unsymmetrically substituted materials of type A generally have lower permeabilities but higher selectivities. Both symmetrically and unsymmetrically substituted units can have severely restricted local motions, as judged by sub-T_g relaxation behavior; however, the lower T_g's observed for materials with type A asymmetrically substituted backbone phenyl rings compared to those containing symmetrically substituted phenyl ring units indicate that longer scale chain rigidity is not similarly affected.[6] There is less available information on the physical and gas transport effects of type B asymmetry; however, one study has shown that when the various substituent groups are all similar in character (i.e., all small alkyl groups), additivity of substituent effects is obtained, at least for polyimides.[5]

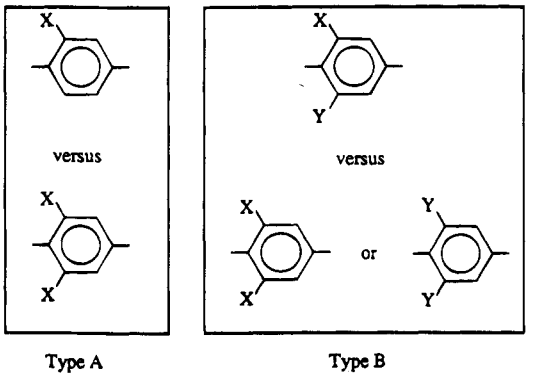

Figure 1. Two possible types of substituted phenyl ring asymmetry. Type A refers to a mono- versus a disubstituted ring, while type B refers to a disubstituted ring where the two substituent groups are not identical.

As a continuation of our previous work,[25–27] this study examines the physical and gas transport properties of a series of homologous polyarylates based on isophthalic acid and various *ortho*-substituted Bisphenol A analogs. Methyl, isopropyl, and bromo substitutions onto the Bisphenol phenyl rings are used to disrupt chain packing and reduce rotational mobility. Our previous work has shown that symmetric bromine substitution of the Bisphenol phenyl rings greatly increases the permselectivity of polyarylates. The latter materials are compared here to the symmetrically methyl-substituted and the type B asymmetrically substituted bromomethyl

[⊗] Abstract published in *Advance ACS Abstracts,* November 1, 1995.

0024-9297/95/2228-8277$09.00/0

Table 1. Monomer Sources and Purification

monomer	abbreviation	source	purification	melting point[a] (°C)
dimethylbisphenol A	DMBPA	Kennedy and Klim	sublimation	139–140
tetramethylbisphenol A	TMBPA	Kennedy and Klim	sublimation	165–167
diisopropylbisphenol A	DiisoBPA	synthesis	recrystallization	98–99
dibromodimethylbisphenol A	DBDMBPA	synthesis	sublimation	120–121
isophthaloyl dichloride	IA	Aldrich	distillation	44–45
5-*tert*-butylisophthaloyl dichloride	tBIA	synthesis	distillation	43–44

[a] After purification.

Table 2. Polyarylate Structures and Physical Properties

structure[a]									
R_1	R_2	R_3	polymer abbreviation	T_g (°C)	T_γ (°C)	ρ (g/cm^3)	d spacing (Å)	FFV[b]	$[\eta]$[c] (dL/g)
CH_3	H	H	DMBPA/IA	165	45	1.180	5.00	0.153	0.48
CH_3	H	*tert*-butyl	DMBPA/tBIA	177	25	1.102	5.12	0.177	0.85
CH_3	CH_3	H	TMBPA/IA	213	47	1.118	5.90	0.174	0.39
CH_3	CH_3	*tert*-butyl	TMBPA/tBIA	231	53	1.055	5.53	0.194	0.42
$-CH(CH_3)_2$	H	H	DiisoBPA/IA	122	−10	1.114	6.14, 4.76	0.168	0.68
$-CH(CH_3)_2$	H	*tert*-butyl	DiisoBPA/tBIA	142	25	1.061	5.21, 9.50	0.184	0.52
CH_3	Br	H	DBDMBPA/IA	233	78	1.448	4.35, 6.60	0.179	0.60
H	H	H	BPA/IA[d]	183	−57	1.212	4.8	0.161	0.85
H	H	*tert*-butyl	BPA/tBIA[d]	218	−63	1.126	5.0, 10.1	0.174	1.13
Br	Br	H	TBBPA/IA[e]	235		1.764	4.2, 3.2, 7.4	0.178	0.47

[a] The general polyarylate structure is

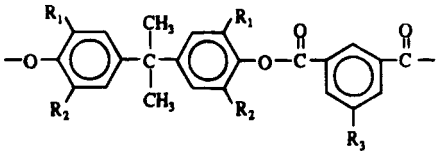

[b] FFV calculated using the methods of Bondi and van Krevelen.[31,32] [c] At 25 °C in chloroform. [d] Data from ref 25. [e] Data from ref 26.

analogs; since methyl and bromo substituents have very similar occupied volumes, property differences probably are related to differences in polarity between bromo and methyl groups. Substitution of tertiary butyl (*tert*-butyl) groups onto the aromatic polymer backbone is used to further disrupt chain packing and increase the permeability of the base material.

Experimental Section

The monomer sources and their purification methods are listed in Table 1. Diisopropyl-Bisphenol A was synthesized by condensing 2-isopropylphenol and acetone in the presence of hydrogen chloride.[28] Dibromodimethyl-Bisphenol A was prepared by direct bromination of dimethyl-Bisphenol A.[29] 5-*tert*-Butylisophthaloyl dichloride was synthesized by refluxing the free acid with an excess of thionyl chloride and then purified by vacuum distillation. The other monomers were obtained commercially. All the polyarylates described in this paper were synthesized in our laboratory via solution polycondensation reactions as outlined by Morgan.[30] The polymer structures and their name abbreviations are listed in Table 2. Each polymer was precipitated at least two times from chloroform or dichloromethane solution into ethanol or methanol and then vacuum dried to remove any residual solvent. The intrinsic viscosity for each polymer was measured in chloroform at 25 °C using a size 25 Cannon-Fenske capillary viscometer. The levels of molecular weight indicated by these values proved to be high enough to form useful films. Data for three analogous polyarylates based on Bisphenol A and tetrabromo-Bisphenol A are included for comparison.[25,26]

Approximately 5 wt % solutions of each polymer in chloroform were cast onto glass plates to give clear films 2–3 mils in thickness. After most of the solvent had evaporated, the films were stripped from the glass plates and vacuum dried, first at room temperature for 24 h and then at incrementally higher temperatures until 150 °C was reached after about 4 days. The films were held above 150 °C for at least 24 h and then removed from the vacuum oven. Those polymers with glass transition temperatures (T_g) below 150 °C were dried at a maximum temperature approximately 10 deg below the polymer T_g. Complete solvent removal was verified by thermogravimetric analysis (TGA) using a Perkin-Elmer TGA-7. Weight loss prior to the onset of polymer degradation was taken as an indication of residual solvent and any suspect films were vacuum dried for an additional 72 h and retested.

The T_g of each polymer was measured using a Perkin-Elmer DSC-7 differential scanning calorimeter (DSC) at a heating rate of 20 °C/min. The samples were heated twice, and the T_g was taken as the midpoint of the heat capacity transition during the second scan. All these polyarylates appear to be amorphous since no crystalline melting points were observed. Dynamic mechanical analysis (DMA) was performed using a Polymer Laboratories DMTA operated at a frequency of 3 Hz and a heating rate of 4 °C/min from −150 to +200 °C. Test bars (~1.5 mm in thickness) were prepared by laminating several strips of each sample film together in a small press, at 15–20 deg above the polymer T_g. The polymer bars were rapidly quenched to room temperature after pressing to standardize the thermal history of each sample.

Wide angle X-ray diffraction (WAXD) spectra for each polymer were made using a Phillips APD 3520 X-ray diffractometer at a Cu Kα wavelength of 1.54 Å. The broad diffraction peak obtained for amorphous polymers can be an indicator of the average chain spacing. The corresponding d spacings were calculated from the diffraction peak maxima using the Bragg equation, $n\lambda = 2d \sin\theta$. Polymer densities were measured in a density gradient column on the basis of degassed, aqueous solutions of calcium nitrate at 30 °C. The polymer densities were used to calculate the fractional free volume (FFV) following the method of Bondi and van Krevelen[31,32]

$$\mathrm{FFV} = \frac{V - V_0}{V} \tag{1}$$

where V is the measured polymer specific volume and V_0 is the occupied volume. The occupied volume was estimated from the van der Waals volume (V_W) according to the relation

$$V_0 = 1.3V_W \quad (2)$$

The factor of 1.3 was estimated from data for only a few polymeric materials and is only an approximation. Quantitative calculation of FFV is difficult; however, interesting qualitative and semiquantitative comparisons have been made between materials with similar structures.

Pure gas permeability coefficients at 35 °C for He, H_2, O_2, N_2, CH_4, and CO_2 gases were measured in a pressure-rise type permeation cell using the standard technique employed in our laboratory.[33] All the gases were chromatography grade with the exception of CH_4 which was chemically pure grade. H_2 and O_2 permeabilities were measured at upstream driving pressures as high as 6 atm while He, N_2, CH_4, and CO_2 permeabilities were measured up to 20 atm. CO_2 permeation was measured last since time-dependent hysteresis has been associated with CO_2 pressurization and depressurization cycles in some materials.[34,35] Ideal permselectivities ($\alpha^*_{A/B}$) were calculated from

$$\alpha^*_{A/B} = P_A/P_B \quad (3)$$

where P_A and P_B are the pure gas A and B permeabilities. If the downstream pressure is negligible and there are no penetrant/penetrant interactions or plasticization of the membrane material, this ideal permselectivity should provide a good estimate of the actual mixed gas performance. Pure gas sorption of O_2 at pressures up to 6 atm and N_2, CH_4, and CO_2 at pressures up to 35 atm was measured in a two-volume pressure decay type sorption cell at 35 °C.[36,37]

Polymer Characterization

The physical properties, as well as structures and nomenclature used, of these polyarylates are listed in Table 2. All the polymers formed clear, tough films with adequate strength for mechanical manipulation. The T_g's of the *tert*-butyl-substituted polymers are higher than those for the unsubstituted analogs; the magnitude of the increase depending upon the size and placement of the various substituent groups. The T_g of DMBPA/tBIA is 12 deg higher than that of DMBPA/IA, the T_g of TMBPA/tBIA is 18 deg higher than that of TMBPA/IA, and the T_g of DiisoBPA/tBIA is 20 deg higher than that of DiisoBPA/IA. Symmetry effects on polymer T_g are readily apparent from Table 2. For both the isophthalate and *tert*-butylisophthalate series, the glass transition temperatures rank as follows:

TMBPA > BPA > DMBPA > DiisoBPA

The four polymers based on the type A asymmetric monomers (DMBPA and DiisoBPA) all have lower T_g's than the unsubstituted BPA/IA material while the three polymers based on the symmetric or type B asymmetric monomers (TMBPA and DBDMBPA) all have higher T_g's. Symmetric methyl group substitution has previously been shown to increase polymer T_g while type A asymmetric methyl group substitution lowers T_g.[6] The T_g of DBDMBPA/IA is only 2 deg lower than that of the symmetrically brominated analog, TBBPA/IA, but 20 deg higher than that of the symmetrically methylated analog, TMBPA/IA. The chain stiffening effect of one bromine substitution is apparently quite similar to that of two. These results confirm that type A asymmetry has a much larger effect on polymer physical properties than type B asymmetry.

The WAXD scans for the various polyarylates are shown in Figure 2; all of these materials are clearly amorphous. The polymers based on DMBPA and TMBPA show only one broad diffraction peak which may be a composite of several overlapping peaks too closely spaced to be resolved; the DiisoBPA-based and DBDMBPA/IA polymers show two broad but distinct diffraction peaks. Two distinct WAXD peaks have been reported for polymers with pendant phenyl rings or aromatic connector groups such as polystyrene,[38,39] fluorene Bisphenol and phenolphthalein isophthalates,[25] and poly(2,6-diphenyl-1,4-phenylene oxide)[2,40] and have been attributed to pendant or connector group "stacking". Since such "stacking" is impossible in the current materials, the secondary diffraction peaks must have some other origin. The secondary peak in the DiisoBPA/tBIA spectra may be a second-order ($n = 2$) diffraction. The much higher X-ray scattering ability of bromine is a likely source of the observed secondary peak in DBDMBPA/IA. The secondary peak in the DiisoBPA/IA spectra is of unknown origin. The most prominent WAXD peak in each spectra was selected as representative of the average polymer chain d spacing and is listed first in the d spacing column of Table 2. Interestingly, the primary d spacings, based on the most prominent WAXD peak, are lower for the *tert*-butyl-substituted TMBPA- and DiisoBPA-based materials than for the unsubstituted analogs. The lower density of the *tert*-butyl-substituted materials suggest that the distance between their chains should be higher. Apparently, the X-ray spectra reflect scattering features other than the average distance between polymer chains and, thus, have limited usefulness for interpreting transport properties.

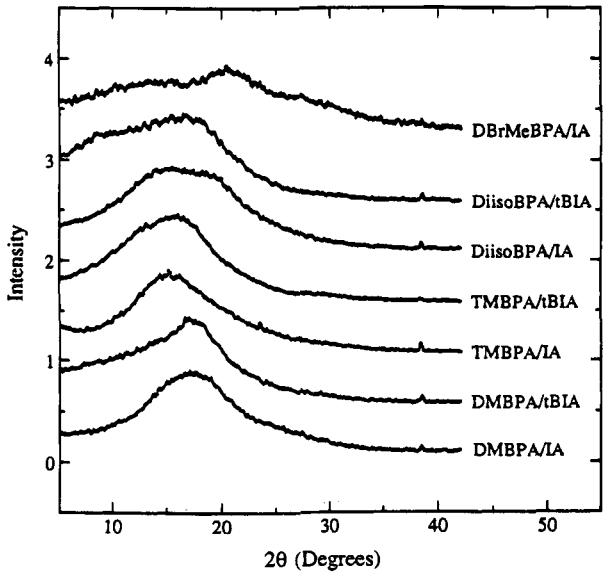

Figure 2. Wide angle X-ray diffraction scans for each of the polyarylates.

The calculated polymer fractional free volumes are listed in Table 2. In every case, FFV is increased by addition of a *tert*-butyl group to the isophthalate unit. The increase in FFV is largest for the polymers based on DMBPA and smallest for those based on DiisoBPA. For either the isophthalate or *tert*-butylisophthalate series the FFV's rank in the following order:

TMBPA > DiisoBPA > DMBPA

The FFV of TMBPA/IA is higher than that of BPA/IA, while that of DMBPA/IA is lower. This compares well with a series of polysulfones synthesized from these same monomers by McHattie.[6] The FFV of DBDMBPA/IA is slightly larger than that of TMBPA/IA and almost identical to that calculated for TBBPA/IA. These results indicate that type A asymmetrically substituted poly-

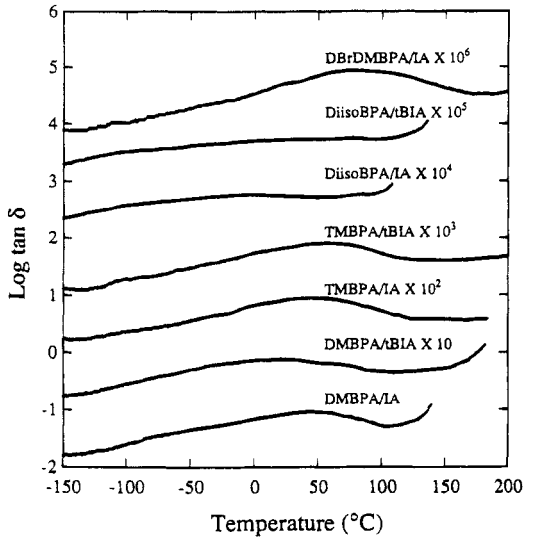

Figure 3. tan δ at 3 Hz as a function of temperature for the polyarylates. The curve for the DMBPA/IA material corresponds to the tan δ scale shown. The curves for all the other polymers have been shifted upward by factors of 10 (for DMBPA/tBIA), 100 (for TMBPA/IA), etc., for clarity.

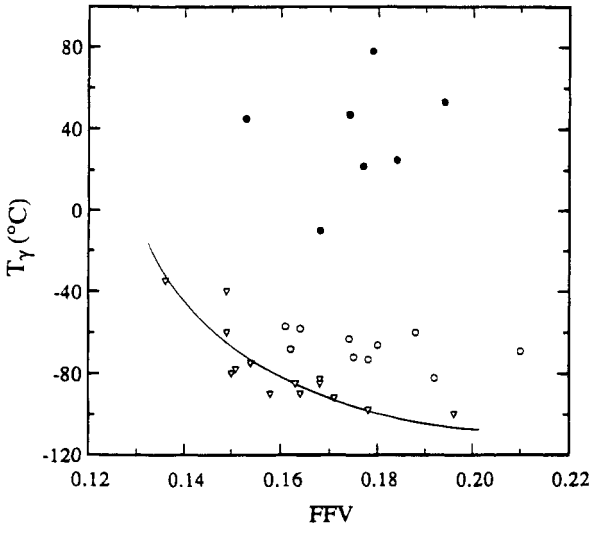

Figure 4. Relationship between the sub-T_g relaxation temperature, T_γ, and fractional free volume. Solid circles represent the current polyarylate data, while the open symbols are for polyarylates (circles) and polysulfones (triangles) described elsewhere. The line represents the best fit of the polysulfone data.

mers pack more efficiently while symmetrically substituted polymers pack less efficiently. This is supported by the higher density of the DMBPA-based polymers as compared to their TMBPA-based analogs. For type B asymmetry, packing is not strongly affected and, thus, DBDMBPA/IA has a FFV between that of TMBPA/IA and TBBPA/IA.

The DMTA traces for these polyarylates are shown in Figure 3; the temperatures at which the sub-T_g γ-relaxation occurs, i.e., T_γ, are summarized in Table 2. For all the polymers, the tan δ peaks are quite broad, much more so than for polyarylates containing unsubstituted Bisphenol phenyl rings. The broadness of the observed relaxation peaks makes the exact determination of the maxima more difficult. The T_γ relaxation maxima occurs 20 deg lower for DMBPA/tBIA than for DMBPA/IA; however, it is 5 deg higher for the TMBPA-based *tert*-butyl isophthalate than for the unsubstituted analog and 35 deg higher in the case of the DiisoBPA-based materials. The highest measured T_γ among the current polyarylates is for DBDMBPA/IA. These differences can be understood in terms of changes in FFV and rotational barriers. The rotational barrier of a substituted phenyl ring is much higher than that of an unsubstituted one, hence, the large shift in T_γ between these polyarylates and the similar but unsubstituted materials reported previously. The *tert*-butyl substitution, which simultaneously increases FFV and hinders phenyl ring rotational mobility through steric interactions, may raise or lower the measured T_γ depending upon which effect is dominant. For the relatively densely packed DMBPA/IA, the lower intermolecular barriers to rotation following *tert*-butyl substitution, due to larger interchain spacings, are the primary cause for the observed decrease in T_γ. For the polymers based on TMBPA and DiisoBPA, increased intrachain steric barriers to phenyl ring rotational mobility following *tert*-butyl substitution dominate. The presence of polar or polarizable groups on the polymer backbone should increase intermolecular attractions and, thus, rotational barriers. This may explain why the T_γ for DBDMBPA/IA is higher than that of TMBPA/IA.

Figure 4 shows a plot of T_γ versus FFV for these polyarylates and a number of other polymers previously reported.[3,4,6-8,25,27] The current polyarylates consistently have T_γ much higher than the other materials having similar FFV. The addition of substituent groups to the Bisphenol phenyl rings more strongly affects rotational mobility than the changes in FFV among the comparison materials, all of which have at least some unsubstituted phenyl rings.

Table 3. Helium Permeability and Ideal Selectivities at 35 °C

polymer	P_{He} (10 atm) (barrer[a])	$\alpha^*(He/CH_4)$[b]	$\alpha^*(He/H_2)$[c]
DMBPA/IA	9.5	207	1.22
DMBPA/tBIA	26	65	0.96
TMBPA/IA	34	72	0.88
TMBPA/tBIA	72	28	0.75
DiisoBPA/IA	19.5	64	1.03
DiisoBPA/tBIA	37.3	26	0.90
DBDMBPA/IA	22.1	146	0.95
BPA/IA[d]	13.4	58	1.00
BPA/tBIA[d]	34.3	24	0.80
TBBPA/IA[e]	16.3	115	0.89

[a] Barrer = 10^{-10} [(cm cm^3(STP))/(cm^2 s cmHg)]. [b] 10 atm. [c] 2 atm. [d] Data from ref 25. [e] Data from ref 26.

Gas Sorption and Transport

Permeation. Pure gas permeability coefficients and ideal selectivities for gas pairs of particular interest are shown in Tables 3–5. Permeability isotherms are given in Figures 5–10 as a function of upstream driving pressure. The permeability coefficients for CO_2, CH_4, and N_2 decrease with increasing upstream pressure while those of He, H_2, and O_2 show little pressure dependence, as expected for glassy polymers. For both the isophthalate and *tert*-butylisophthalate-based polyarylates described here, the permeabilities to the various gases fall in the following order within each series of fixed Bisphenol unit.

TMBPA > DiisoBPA > DMBPA

For both the *tert*-butyl-substituted and unsubstituted series the DMBPA-based polymers have higher He/CH_4, CO_2/CH_4, and O_2/N_2 selectivities than either the

Table 4. Mobility and Solubility Components of the O_2/N_2 Separation Factor[a]

polymer	P_{O_2} [barrer]	$\alpha^*(O_2/N_2)$	$\bar{S}_{O_2}$[b] [cm³ (STP) cm⁻³ atm⁻¹]	$\bar{S}_{O_2}/\bar{S}_{N_2}$	$10^8\bar{D}_{O_2}$[c] [cm²/s]	$\bar{D}_{O_2}/\bar{D}_{N_2}$
DMBPA/IA	0.40	6.37	0.33	1.33	0.93	4.78
DMBPA/tBIA	2.37	6.03	0.42	1.31	4.31	4.61
TMBPA/IA	3.26	5.63	0.55	1.37	4.53	4.11
TMBPA/tBIA	12.2	4.84	0.74	1.26	12.5	3.82
DiisoBPA/IA	1.64	6.01	0.17	1.66	7.33	3.62
DiisoBPA/tBIA	5.03	4.66	0.25	1.55	15.5	3.01
DBDMBPA/IA	1.52	6.94	0.59	1.25	1.94	5.54
BPA/IA[d]	1.33	5.54	0.28	1.92	3.62	2.89
BPA/tBIA[d]	5.95	4.97	0.50	1.48	9.06	3.34
TBBPA/IA[e]	1.30	7.23	0.45	1.77	2.19	4.11

[a] Data at 35 °C and 2 atm. [b] Calculated from the sorption isotherm. [c] Calculated from $D = P/S$. [d] Data from ref 25. [e] Data from ref 26.

Table 5. Mobility and Solubility Components of the CO_2/CH_4 Separation Factor[a]

polymer	P_{CO_2} [barrer]	$\alpha^*(CO_2/CH_4)$	$\bar{S}_{CO_2}$[b] [cm³ (STP) cm⁻³ atm⁻¹]	$\bar{S}_{CO_2}/\bar{S}_{CH_4}$	$10^8\bar{D}_{CO_2}$ [cm²/s][c]	$\bar{D}_{CO_2}/\bar{D}_{CH_4}$
DMBPA/IA	1.24	27	1.70	3.10	0.55	8.70
DMBPA/tBIA	8.0	20	2.23	2.93	2.74	6.81
TMBPA/IA	12.0	25.3	2.73	2.83	3.35	8.94
TMBPA/tBIA	44.6	17.4	3.04	2.80	11.2	6.19
DiisoBPA/IA	5.16	17.0	1.53	4.13	2.57	4.12
DiisoBPA/tBIA	16.1	11.4	1.70	3.15	7.18	3.63
DBDMBPA/IA	5.45	36.1	2.76	2.73	1.50	13.2
BPA/IA[d]	5.4	23.2	1.73	3.91	2.38	5.93
BPA/tBIA[d]	24.2	16.9	2.52	2.92	7.30	5.79
TBBPA/IA[e]	4.93	34.7	1.81	2.62	2.07	13.2

[a] Data at 35 °C and 10 atm. [b] Calculated from the sorption isotherm. [c] Calculated from $D = P/S$. [d] Data from ref 25. [e] Data from ref 26.

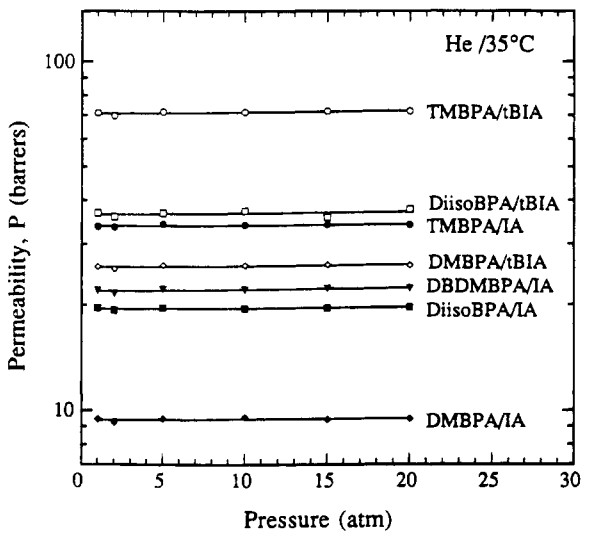

Figure 5. Pressure dependence of He permeability coefficients at 35 °C.

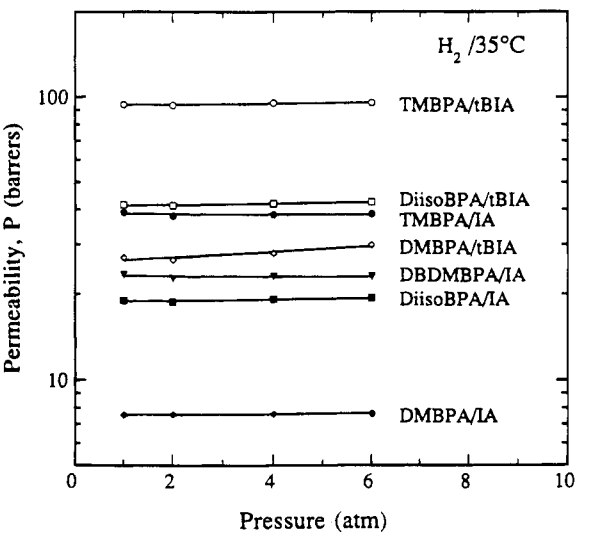

Figure 6. Pressure dependence of H_2 permeability coefficients at 35 °C.

TMBPA or DiisoBPA-based analogs. DBDMBPA/IA has the highest O_2/N_2 and CO_2/CH_4 selectivities of any new polymer reported here; however, its selectivity for O_2/N_2 is lower than that of the previously reported TBBPA,[26] whose results are also shown here for comparison. The He/CH_4 and CO_2/CH_4 selectivities of DBDMBPA/IA are higher than those of TBBPA/IA. The TMBPA-based polymers have permselectivities similar to their BPA-based analogs but at higher levels of permeability. All of the substituted polymers in this study have either higher permeability, higher selectivity, or both than the unsubstituted comparison polymer BPA/IA.

The *tert*-butyl-substituted materials have higher gas permeabilities than their unsubstituted analogs; the magnitude of the increase is larger the smaller the size and number of the Bisphenol substituent groups. *tert*-Butyl substitution increases the permeability by approximately 2–3-fold for He and H_2 and by 3–6-fold for N_2, O_2, CH_4, and CO_2. The calculated ideal selectivities are lower for all gas pairs in the *tert*-butyl-substituted materials, as expected from the well-known "trade-off" relation.

The effects of substitutions on the phenyl rings on the O_2/N_2 selectivity versus O_2 permeability "trade-off" are shown graphically in the top portion of Figure 11. The symmetrically methylated material, TMBPA/IA, has a higher O_2 permeability and a slightly higher O_2/N_2 selectivity than the unsubstituted BPA/IA. Type A asymmetric methyl substitution, i.e. DMBPA/IA, yields a material with lower O_2 permeability but higher O_2/N_2 selectivity than BPA/IA while type A asymmetric isopropyl substitution, i.e. DiisoBPA/IA, yields a material with both slightly higher O_2 permeability and O_2/N_2 selectivity. The type B asymmetrically substituted material, DBDMBPA/IA, has similar O_2 permeability but much higher O_2/N_2 selectivity than BPA/IA and is much closer to TBBPA/IA than TMBPA/IA in transport

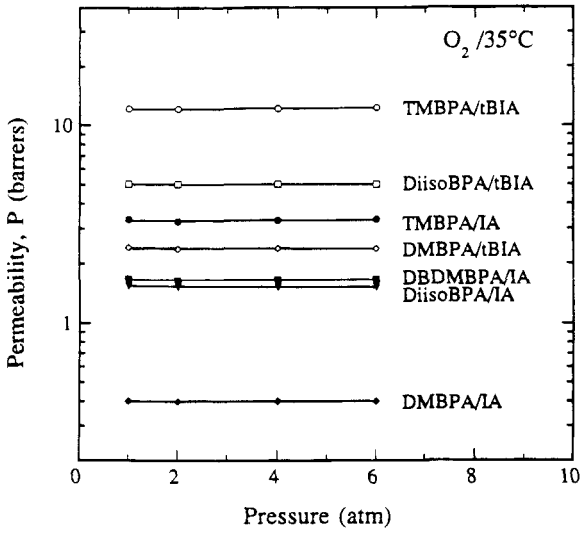

Figure 7. Pressure dependence of O_2 permeability coefficients at 35 °C.

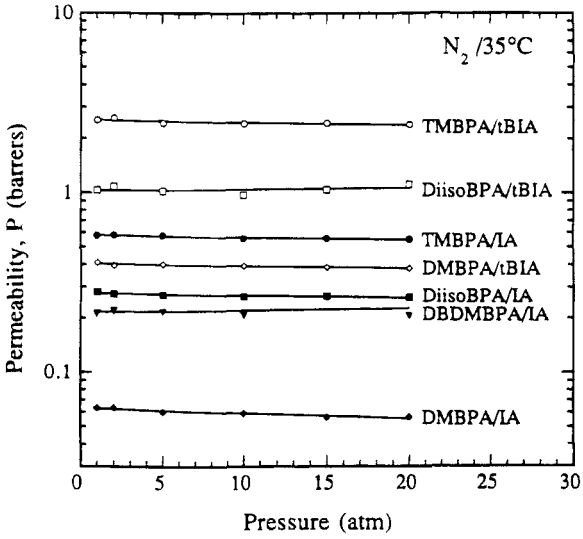

Figure 8. Pressure dependence of N_2 permeability coefficients at 35 °C.

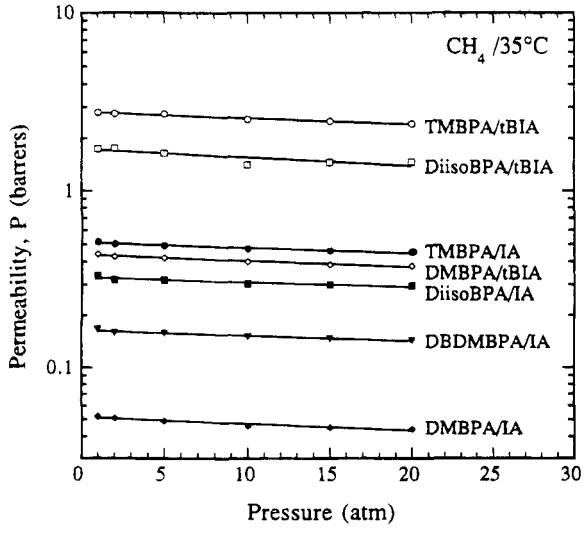

Figure 9. Pressure dependence of CH_4 permeability coefficients at 35 °C.

properties. The effect of *tert*-butyl substitution can be seen in the bottom section of Figure 11. *tert*-Butyl substitution moves most of the polymers parallel to the

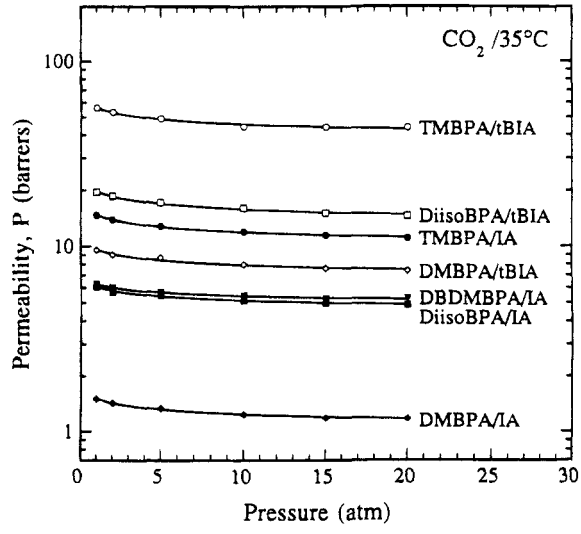

Figure 10. Pressure dependence of CO_2 permeability coefficients at 35 °C.

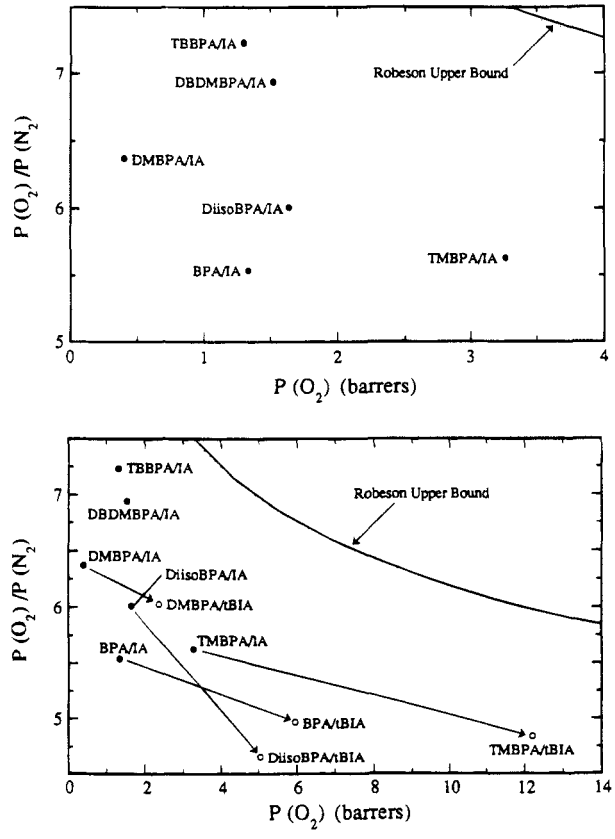

Figure 11. Effect of monomer structure on the oxygen permeability and oxygen/nitrogen selectivity for the various isophthalates (upper plot) and *tert*-butyl-substituted isophthalates (lower plot) where solid points represent isophthalates and open points represent *tert*-butyl isophthalates. The curve in the upper right of both plots is the "upper bound" as proposed by Robeson.[22]

Robeson upper bound curve with the exception of the DiisoBPA material which moves slightly away.

Figure 12 shows the permeability coefficient for DBDMBPA/IA divided by that for TMBPA/IA as a function of upstream pressure for all the gases. Note that each of the permeability ratios is significantly less than 1, indicating the lower permeability of DBDMBPA/IA. The calculated permeability ratio for He is approximately twice that of CH_4; thus, He/CH_4 selectivity is much higher for the brominated material. Similarly,

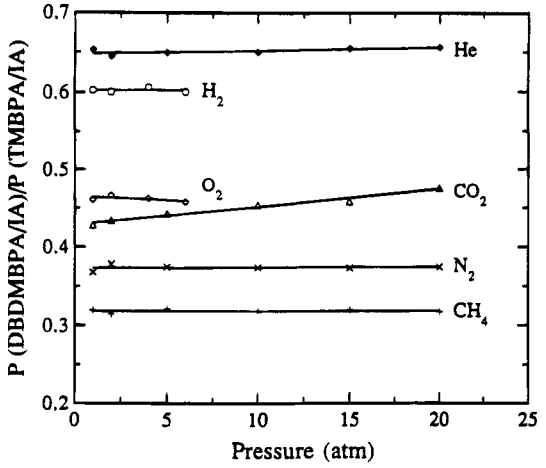

Figure 12. Ratio of the permeability coefficients for DBDMBPA/IA divided by those of TMBPA/IA for various gases as a function of pressure at 35 °C.

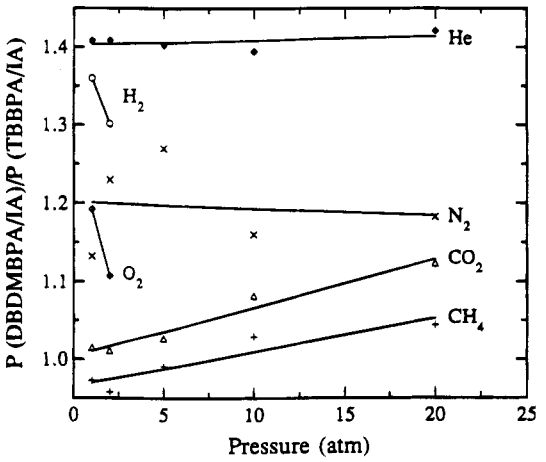

Figure 13. Ratio of the permeability coefficients for DBDMBPA/IA divided by those of TBBPA/IA for various gases as a function of pressure at 35 °C.

the permeability ratio for O_2 is higher than that of N_2; hence, the O_2/N_2 selectivity of DBDMBPA/IA is higher than that of TMBPA/IA. This evidence suggests that DBDMBPA/IA is more size selective than TMBPA/IA which may result from the stiffening effect of enhanced polar interactions between chains. Figure 13 shows a similar plot of the permeability coefficient for DBDMBPA/IA divided by that for TBBPA/IA. Note that in this case the permeability ratios are all near to or greater than 1. The permeability ratio is highest for He and declines with penetrant molecular size. The scatter of the N_2 permeability ratio data is mainly due to small measurement errors which are most significant for the gases which permeate slowly, i.e., N_2 and CH_4.

Previous studies have shown an approximate correlation between gas permeability, P, and fractional free volume, FFV, of the form

$$P = A \exp\left(\frac{-B}{\mathrm{FFV}}\right) \tag{4}$$

where the parameters A and B depend only on temperature and gas type. A semilogarithmic plot of O_2 permeability versus inverse FFV is shown in Figure 14 for these polyarylates along with data for a number of other polymers. The polyarylate data tend to fall somewhat below the best fit line for the polysulfone data; however, these differences may reflect inaccuracies

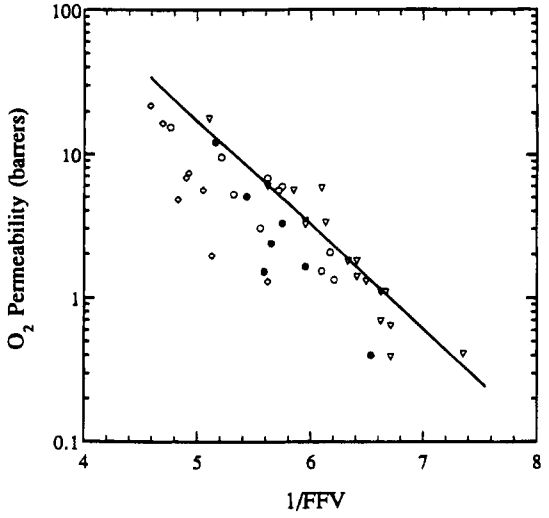

Figure 14. Correlation of oxygen permeability with inverse fractional free volume. Solid points represent the current polyarylate data, while open points correspond to various other polyarylates (circles), brominated polyarylates (diamonds), and polysulfones (triangles) described elsewhere. The line is the best linear fit to the polysulfone data.

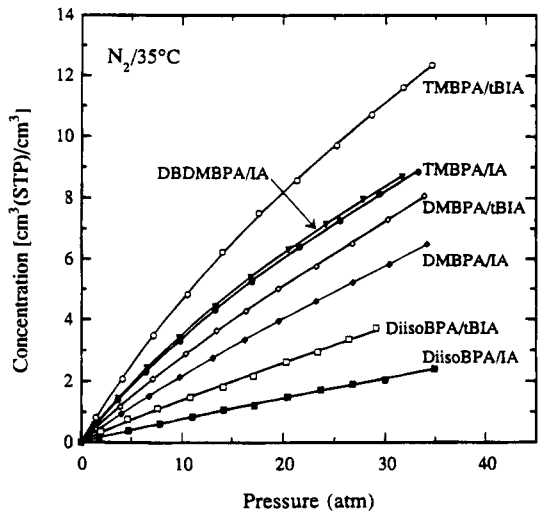

Figure 15. Sorption isotherms for nitrogen at 35 °C. Solid points represent the unsubstituted materials, while open points represent the *tert*-butyl-substituted analogs.

in the calculated van der Waals volumes for certain groups. Additionally, it has been suggested that some of the effects associated with polarity may not be fully accounted for in this approach, which may explain the deviation of a number of the brominated polymer materials from this correlation.[7]

Sorption. Pure gas sorption isotherms for N_2, CH_4, and CO_2 are shown in Figures 15–17 for this series of polyarylates. For a given polymer, CO_2 sorption is highest followed by that of CH_4 and N_2. Note that the gas sorption isotherms for TMBPA/IA and DBDMBPA/IA are virtually identical. The relative contributions of solubility and diffusivity to the overall gas permeability can be determined from

$$P = \bar{D}\bar{S} \tag{5}$$

where $\bar{D}$ is the concentration-averaged diffusion coefficient and $\bar{S}$ is the solubility coefficient calculated from the secant slope of the sorption isotherm evaluated at the upstream condition. The ideal overall permselectivity (eq 3) can be factored into solubility and diffusivity

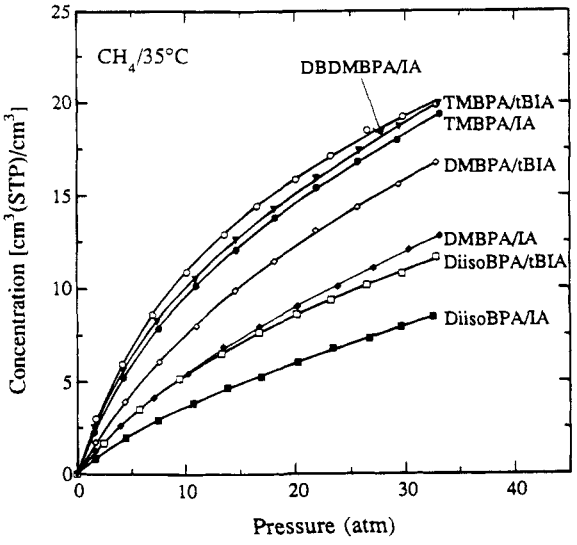

Figure 16. Sorption isotherms for methane at 35 °C. Solid points represent the unsubstituted materials, while open points represent the *tert*-butyl-substituted analogs.

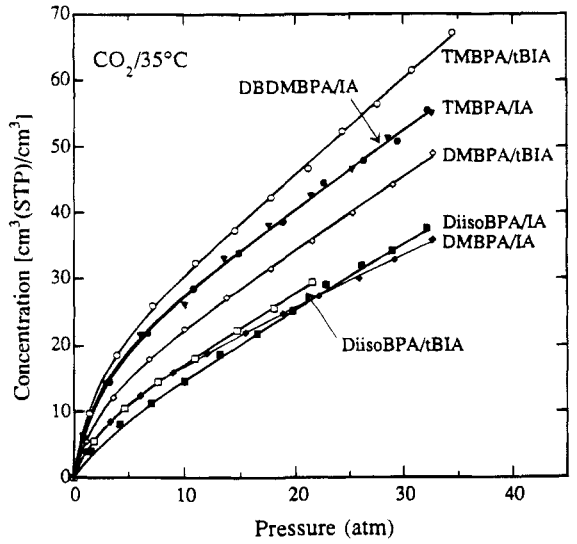

Figure 17. Sorption isotherms for carbon dioxide at 35 °C. Solid points represent the unsubstituted materials, while open points represent the *tert*-butyl-substituted analogs.

terms using eq 5 to give

$$\alpha^*_{A/B} = \frac{P_A}{P_B} = \left(\frac{\bar{D}_A}{\bar{D}_B}\right)\left(\frac{\bar{S}_A}{\bar{S}_B}\right) \qquad (6)$$

where $(\bar{D}_A/\bar{D}_B)$ is the mobility selectivity and $(\bar{S}_A/\bar{S}_B)$ is the solubility selectivity. The O_2 and CO_2 solubility and diffusivity coefficients as well as the calculated solubility and mobility selectivities for the gas pairs O_2/N_2 and CO_2/CH_4 are reported in Tables 4 and 5.

Oxygen solubility is highest in the TMBPA and DBDMBPA-based polymers and lowest in the DiisoBPA-based polymers, while the DMBPA-based polymers fall in between. Oxygen diffusivity is highest for the DiisoBPA- and TMBPA-based polymers and is much lower for those based on DMBPA and DBDMBPA. The well-packed chains of the DMBPA-based polymers and the interchain polar interaction of DBDMBPA/IA are probably responsible for their low O_2 diffusivities. *tert*-Butyl substitution increases both the O_2 solubility and O_2 diffusivity coefficients of the TMBPA-, DMBPA-, and

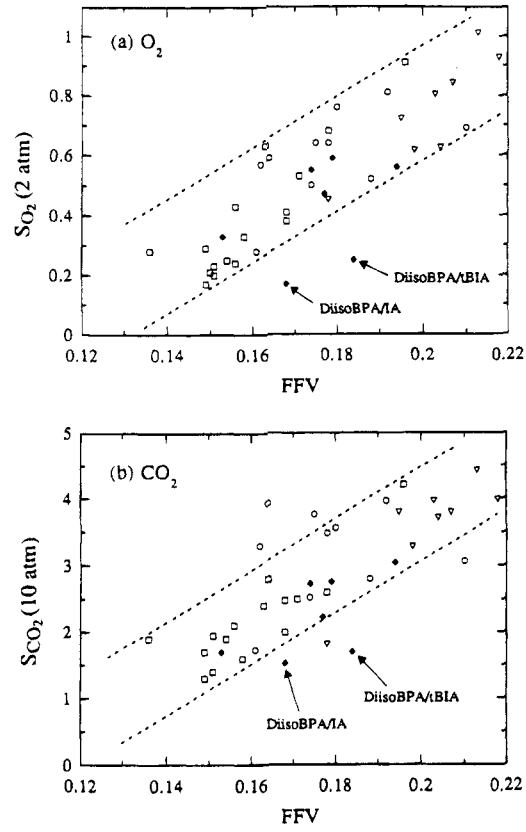

Figure 18. Correlation of the O_2 (a) and CO_2 (b) solubility coefficient at 35 °C with fractional free volume. Diamonds represent the polyarylates reported here, while open points correspond to polyarylates (circles), brominated polyarylates (triangles), and polysulfones (squares) described elsewhere. The dotted lines represent the approximate boundaries of the polymer data.

DiisoBPA-based materials. *tert*-Butyl substitution generally decreases O_2/N_2 diffusivity and solubility selectivity so that the overall selectivity declines. Note that the oxygen solubility levels in DBDMBPA/IA are similar to those observed for TMBPA/IA and are higher than in TBBPA/IA.

Carbon dioxide solubility is highest for the TMBPA- and DBDMBPA-based materials, intermediate for those based on DMBPA, and lowest for the DiisoBPA-based polymers. Carbon dioxide diffusivity is highest for the TMBPA-based polymers, intermediate for those based on DiisoBPA, and lowest for those based on DMBPA and DBDMBPA. The CO_2/CH_4 solubility selectivity follows a trend opposite that of CO_2 solubility. *tert*-Butyl substitution increases CO_2 solubility; however, the 3–4-fold increases in CO_2 diffusivity are the largest factor in the increased CO_2 permeabilities. *tert*-Butyl substitution causes both the solubility and the diffusivity selectivities for CO_2/CH_4 to decline so that the ideal CO_2/CH_4 selectivities for the *tert*-butyl-substituted materials are somewhat lower. The solubility levels for N_2 and CH_4 follow similar trends according to connector group size, with the order being TMBPA > DMBPA > DiisoBPA.

Changes in polymer FFV can explain some of the effects of *tert*-butyl and connector group substitutions on gas sorption. Polymers with high FFV tend to have high gas sorption levels. Figure 18 shows the effect of FFV on the gas sorption capacity, S, of O_2 (at 2 atm) and CO_2 (at 10 atm) where S is calculated from the secant slope of the sorption isotherm. For oxygen, most of the polyarylate values fall within the band, defined

Table 6. Dual-Mode Sorption Parameters at 35 °C

polymer	gas	k_D [cm³ (STP) cm⁻³ atm⁻¹]	C'_H [cm³ (STP) cm⁻³]	b [atm⁻¹]
DMBPA/IA	N_2	0.160	1.43	0.069
	CH_4	0.230	7.12	0.081
	CO_2	0.714	13.71	0.252
DMBPA/tBIA	N_2	0.192	2.21	0.065
	CH_4	0.326	7.90	0.114
	CO_2	1.062	14.83	0.366
TMBPA/IA	N_2	0.182	4.42	0.054
	CH_4	0.252	14.51	0.096
	CO_2	1.118	20.62	0.354
TMBPA/tBIA	N_2	0.231	6.59	0.061
	CH_4	0.261	15.3	0.117
	CO_2	1.39	19.75	0.502
DiisoBPA/IA	N_2	0.058	0.54	0.097
	CH_4	0.168	4.01	0.101
	CO_2	0.975	7.12	0.287
DiisoBPA/tBIA	N_2	0.110	0.613	0.096
	CH_4	0.190	7.12	0.097
	CO_2	0.952	10.09	0.324
DBDMBPA/IA	N_2	0.139	6.84	0.055
	CH_4	0.280	13.51	0.118
	CO_2	1.102	20.72	0.401

by the two dashed lines in Figure 18, occupied by a large number of polymers studied previously; the exceptions being the much lower levels of solubility exhibited by the two polymers based on DiisoBPA. For carbon dioxide, some of the polyarylate values fall within a similar band (see Figure 18) containing the other polymer data; however, the two DiisoBPA-based materials again show substantially lower solubility coefficients. Positive deviations of CO_2 solubility from this type of rough correlation have been observed for some polymers examined previously and have been related to the high concentration of carbonyl groups in these materials. The low gas solubility levels shown here for the DiisoBPA-based materials, at least in part, may be related to their low T_g's, as explained below.

The sorption data are well described by the dual-mode sorption model[41,42]

$$C = k_D p + \frac{C'_H b p}{1 + bp} \tag{7}$$

where k_D is the Henry's law solubility coefficient, C'_H is the Langmuir capacity factor, and b is an affinity parameter characterizing the relative rates of sorption and desorption. Nonlinear curve fitting of the sorption data to the dual-mode sorption model using the Levenberg–Marquardt algorithm allows calculation of all three model parameters for the gases N_2, CH_4, and CO_2; see Table 6. For all polymers, k_D and C'_H are highest for CO_2 and lowest for N_2 with CH_4 falling in between. Note that the Langmuir capacities of the DiisoBPA-based polymers are considerably lower, for each gas, than those of the other materials in this study while the Henry's law coefficients are all similar. For polymer glasses, the Langmuir contribution to total gas sorption capacity is inversely proportional to the difference between the temperature of sorption and the polymer T_g and, thus, is smaller for polymers with low T_g's.[43] This may explain the low solubility of gases in the DiisoBPA-based materials, but comparison of the k_D values in Table 6 reveals that this is not the only issue involved.

Conclusions

Symmetric and asymmetric replacement of the *ortho* hydrogens on the phenylene rings of the Bisphenol monomer by methyl, isopropyl, or bromo substituents significantly affects the physical and gas transport properties of aromatic isophthalates. Dimethyl substitution of each of the Bisphenol phenyl rings (i.e. TMBPA) increases polymer permeability while lowering permselectivity, as compared with the BPA-based analogs. Monomethyl substitution of each of the Bisphenol phenyl rings gives materials that are more selective but less permeable than the BPA-based analogs while monoisopropyl substitution of both Bisphenol phenyl rings gives materials that have similar permeabilities but lower selectivities. Simultaneous bromo and methyl substitution on each of the Bisphenol phenyl rings gives a material very similar in physical and gas transport properties to the symmetrically brominated analog. This observation indicates that polymers with lower bromine contents can achieve membrane performance nearly equivalent to that of the highly attractive tetrabrominated materials discussed earlier;[26] potential implications of this in terms of polymer synthesis, economics, stability, etc. should be explored. Substitution of a *tert*-butyl group at position 5 of the isophthalate unit increases gas permeability by 2–6-fold, depending upon the gas, while decreasing permselectivity. Gas sorption is moderately increased in all cases by *tert*-butyl substitution and by symmetric bisphenol ring substitution; however, increased diffusion coefficients are the primary cause of the much higher gas permeabilities.

The selectivity enhancing ability of the bromine substitution appears to result from both size and polarity considerations. Interchain polar attractions stiffen the polymer backbone, increasing permselectivity, while packing constraints prevent a collapse of free volume and concomitant loss of permeability. The incorporation of polar or polarizable groups within polymer structures which inhibit free volume collapse appears to be a viable strategy for simultaneously increasing permeability and permselectivity.

Acknowledgment. This research was supported by the Department of Energy, Basic Sciences Program, under Grant DE-FG05-86ER13507 and the Separations Research Program at The University of Texas at Austin. M.R.P. acknowledges the Phillips Petroleum Foundation for fellowship support.

References and Notes

(1) Aguilar-Vega, M.; Paul, D. R. *J. Polym. Sci., Polym. Phys. Ed.* **1993**, *31*, 1599.
(2) Aguilar-Vega, M.; Paul, D. R. *J. Polym. Sci., Polym. Phys. Ed.* **1993**, *31*, 1577.
(3) Aitken, C. L.; Koros, W. J.; Paul, D. R. *Macromolecules* **1992**, *25*, 3424.
(4) Aitken, C. L.; Koros, W. J.; Paul, D. R. *Macromolecules* **1992**, *25*, 3651.
(5) Langsam, M.; Burgoyne, W. F. *J. Polym. Sci., Polym. Chem. Ed.* **1993**, *31*, 909.
(6) McHattie, J. S.; Koros, W. J.; Paul, D. R. *Polymer* **1991**, *32*, 840.
(7) McHattie, J. S.; Koros, W. J.; Paul, D. R. *Polymer* **1991**, *32*, 2618.
(8) McHattie, J. S.; Koros, W. J.; Paul, D. R. *Polymer* **1992**, *33*, 1701.
(9) McHattie, J. S.; Koros, W. J.; Paul, D. R. *J. Polym. Sci., Polym. Phys. Ed.* **1991**, *29*, 731.
(10) Tanaka, K.; Kita, H.; Okano, M.; Okamoto, K. *Polymer* **1992**, *33*, 585.
(11) Tanaka, K.; Kita, H.; Okamoto, K.; Nakamura, A.; Kusuki, Y. *J. Membr. Sci.* **1989**, *47*, 203.
(12) Sheu, F. R.; Chern, R. T. *J. Polym. Sci., Polym. Phys. Ed.* **1989**, *27*, 1121.
(13) Weinkauf, D. H.; Paul, D. R. *Macromolecules* **1992**, *25*, 788.
(14) Mohr, J. M.; Paul, D. R. *J. Appl. Polym. Sci.* **1991**, *42*, 1711.

(15) Coleman, M. R. Ph.D. Dissertation, The University of Texas at Austin, 1992.
(16) Hellums, M. W.; Koros, W. J.; Husk, G. R.; Paul, D. R. *J. Appl. Polym. Sci.* **1991**, *43*, 1977.
(17) Kim, T. H.; Koros, W. J.; Husk, G. R.; O'Brien, K. C. *J. Membr. Sci.* **1988**, *37*, 45.
(18) Stern, S. A.; Mi, Y.; Yamamoto, H. *J. Polym. Sci., Polym. Phys. Ed.* **1989**, *27*, 1887.
(19) Ichiraku, Y.; Stern, S. A. *J. Membr. Sci.* **1987**, *34*, 5.
(20) Plate, N. A.; Yampol'skii, Y. P. In *Polymeric Gas Separation Membranes*; Paul, D. R., Yampol'skii, Y. P., Eds.; CRC Press: Boca Raton, FL, 1994; p 155.
(21) Pixton, M. R.; Paul, D. R. In *Polymeric Gas Separation Membranes*; Paul, D. R., Yampol'skii, Y. P., Eds.; CRC Press: Boca Raton, FL, 1994; p 83.
(22) Robeson, L. M. *J. Membr. Sci.* **1991**, *62*, 165.
(23) Koros, W. J.; Story, B. J.; Jordan, S. M.; O'Brien, K.; Husk, G. R. *Polym. Eng. Sci.* **1987**, *27*, 603.
(24) Hellums, M. W.; Koros, W. J.; Husk, G. R.; Paul, D. R. *J. Membr. Sci.* **1989**, *46*, 93.
(25) Pixton, M. R.; Paul, D. R. *J. Polym. Sci., Polym. Phys. Ed.*, in press.
(26) Pixton, M. R.; Paul, D. R. *J. Polym. Sci., Polym. Phys. Ed.*, in press.
(27) Pixton, M. R.; Paul, D. R. *Polymer*, in press.
(28) Schnell, H.; Krimm, H. *Angew. Chem., Int. Ed. Engl.* **1963**, *2*, 373.
(29) Islam, A. M.; Hassan, E. A.; Rashad, M. E.; Wassel, M. M. *Egypt. J. Chem.* **1977**, *20*, 483.
(30) Morgan, P. W. In *Polymer Reviews*: Mark, H. F., Immergut, E. H., Eds.; Interscience Publishers: New York, 1965; p 325.
(31) Bondi, A. *Physical Properties of Molecular Crystals, Liquids, and Glasses*; John Wiley & Sons, Inc.: New York, 1968.
(32) Van Krevelen, D. W. *Properties of Polymers*, 3rd ed.; Elsevier Science Publishers: New York, 1990.
(33) Koros, W. J.; Paul, D. R.; Rocha, A. A. *J. Polym. Sci., Polym. Phys. Ed.* **1976**, *14*, 687.
(34) Jordan, S. M.; Koros, W. J.; Fleming, G. K. *J. Membr. Sci.* **1987**, *30*, 191.
(35) Raymond, P. C.; Paul, D. R. *J. Polym. Sci., Polym. Phys. Ed.* **1990**, *28*, 2213.
(36) Koros, W. J.; Chan, A. H.; Paul, D. R. *J. Membr. Sci.* **1977**, *2*, 165.
(37) Koros, W. J.; Paul, D. R. *J. Polym. Sci., Polym. Phys. Ed.* **1976**, *14*, 1903.
(38) Mitchell, G. R.; Windle, A. H. *Polymer* **1984**, *25*, 906.
(39) Windle, A. H. *Pure Appl. Chem.* **1985**, *57*, 1627.
(40) Wrasidlo, W. *Macromolecules* **1971**, *4*, 642.
(41) Barrer, R. M.; Barrie, J. A.; Slater, J. *J. Polym. Sci.* **1958**, *27*, 177.
(42) Vieth, W. R.; Howell, J. M.; Hsieh, J. H. *J. Membr. Sci.* **1976**, *1*, 177.
(43) Koros, W. J.; Paul, D. R. *J. Polym. Sci., Polym. Phys. Ed.* **1978**, *16*, 1947.

MA950254I